Azimuthal Harmonics in Small and Large Collision Systems at RHIC Top Energies

J. Adam *et al.* (STAR Collaboration)

Azimuthal harmonics in small and large collision systems at RHIC top energies

J. Adam,[12] L. Adamczyk,[2] J. R. Adams,[35] J. K. Adkins,[26] G. Agakishiev,[24] M. M. Aggarwal,[37] Z. Ahammed,[57]
I. Alekseev,[3, 31] D. M. Anderson,[51] R. Aoyama,[54] A. Aparin,[24] D. Arkhipkin,[5] E. C. Aschenauer,[5] M. U. Ashraf,[53]
F. Atetalla,[25] A. Attri,[37] G. S. Averichev,[24] X. Bai,[10] V. Bairathi,[32] K. Barish,[9] A. J. Bassill,[9] A. Behera,[49]
R. Bellwied,[19] A. Bhasin,[23] A. K. Bhati,[37] J. Bielcik,[13] J. Bielcikova,[34] L. C. Bland,[5] I. G. Bordyuzhin,[3]
J. D. Brandenburg,[42] A. V. Brandin,[31] D. Brown,[28] J. Bryslawskyj,[9] I. Bunzarov,[24] J. Butterworth,[42]
H. Caines,[60] M. Calderón de la Barca Sánchez,[7] D. Cebra,[7] I. Chakaberia,[25, 46] P. Chaloupka,[13] B. K. Chan,[8]
F-H. Chang,[33] Z. Chang,[5] N. Chankova-Bunzarova,[24] A. Chatterjee,[57] S. Chattopadhyay,[57] J. H. Chen,[47]
X. Chen,[45] X. Chen,[21] J. Cheng,[53] M. Cherney,[12] W. Christie,[5] G. Contin,[27] H. J. Crawford,[6] M. Csanad,[15]
S. Das,[10] T. G. Dedovich,[24] I. M. Deppner,[18] A. A. Derevschikov,[39] L. Didenko,[5] C. Dilks,[38] X. Dong,[27]
J. L. Drachenberg,[1] J. C. Dunlop,[5] L. G. Efimov,[24] N. Elsey,[59] J. Engelage,[6] G. Eppley,[42] R. Esha,[8] S. Esumi,[54]
O. Evdokimov,[11] J. Ewigleben,[28] O. Eyser,[5] R. Fatemi,[26] S. Fazio,[5] P. Federic,[34] P. Federicova,[13] J. Fedorisin,[24]
P. Filip,[24] E. Finch,[48] Y. Fisyak,[5] C. E. Flores,[7] L. Fulek,[2] C. A. Gagliardi,[51] T. Galatyuk,[14] F. Geurts,[42]
A. Gibson,[56] D. Grosnick,[56] D. S. Gunarathne,[50] Y. Guo,[25] A. Gupta,[23] W. Guryn,[5] A. I. Hamad,[25] A. Hamed,[51]
A. Harlenderova,[13] J. W. Harris,[60] L. He,[40] S. Heppelmann,[7] S. Heppelmann,[38] N. Herrmann,[18] A. Hirsch,[40]
L. Holub,[13] Y. Hong,[27] S. Horvat,[60] B. Huang,[11] H. Z. Huang,[8] S. L. Huang,[49] T. Huang,[33] X. Huang,[53]
T. J. Humanic,[35] P. Huo,[49] G. Igo,[8] W. W. Jacobs,[20] A. Jentsch,[52] J. Jia,[5, 49] K. Jiang,[45] S. Jowzaee,[59]
X. Ju,[45] E. G. Judd,[6] S. Kabana,[25] S. Kagamaster,[28] D. Kalinkin,[20] K. Kang,[53] D. Kapukchyan,[9] K. Kauder,[5]
H. W. Ke,[5] D. Keane,[25] A. Kechechyan,[24] D. P. Kikoλa,[58] C. Kim,[9] T. A. Kinghorn,[7] I. Kisel,[16] A. Kisiel,[58]
L. Kochenda,[31] L. K. Kosarzewski,[58] A. F. Kraishan,[50] L. Kramarik,[13] L. Krauth,[9] P. Kravtsov,[31] K. Krueger,[4]
N. Kulathunga,[19] L. Kumar,[37] R. Kunnawalkam Elayavalli,[59] J. Kvapil,[13] J. H. Kwasizur,[20] R. Lacey,[49]
J. M. Landgraf,[5] J. Lauret,[5] A. Lebedev,[5] R. Lednicky,[24] J. H. Lee,[5] C. Li,[45] W. Li,[47] X. Li,[45] Y. Li,[53]
Y. Liang,[25] J. Lidrych,[13] T. Lin,[51] A. Lipiec,[58] M. A. Lisa,[35] F. Liu,[10] H. Liu,[20] P. Liu,[49] P. Liu,[47] Y. Liu,[51]
Z. Liu,[45] T. Ljubicic,[5] W. J. Llope,[59] M. Lomnitz,[27] R. S. Longacre,[5] S. Luo,[11] X. Luo,[10] G. L. Ma,[47] L. Ma,[17]
R. Ma,[5] Y. G. Ma,[47] N. Magdy,[49] R. Majka,[60] D. Mallick,[32] S. Margetis,[25] C. Markert,[52] H. S. Matis,[27]
O. Matonoha,[13] J. A. Mazer,[43] K. Meehan,[7] J. C. Mei,[46] N. G. Minaev,[39] S. Mioduszewski,[51] D. Mishra,[32]
B. Mohanty,[32] M. M. Mondal,[22] I. Mooney,[59] D. A. Morozov,[39] Md. Nasim,[8] J. D. Negrete,[9] J. M. Nelson,[6]
D. B. Nemes,[60] M. Nie,[47] G. Nigmatkulov,[31] T. Niida,[59] L. V. Nogach,[39] T. Nonaka,[10] G. Odyniec,[27] A. Ogawa,[5]
K. Oh,[41] S. Oh,[60] V. A. Okorokov,[31] D. Olvitt Jr.,[50] B. S. Page,[5] R. Pak,[5] Y. Panebratsev,[24] B. Pawlik,[36]
H. Pei,[10] C. Perkins,[6] R. L. Pinter,[15] J. Pluta,[58] J. Porter,[27] M. Posik,[50] N. K. Pruthi,[37] M. Przybycien,[2]
J. Putschke,[59] A. Quintero,[50] S. K. Radhakrishnan,[27] S. Ramachandran,[26] R. L. Ray,[52] R. Reed,[28] H. G. Ritter,[27]
J. B. Roberts,[42] O. V. Rogachevskiy,[24] J. L. Romero,[7] L. Ruan,[5] J. Rusnak,[34] O. Rusnakova,[13] N. R. Sahoo,[51]
P. K. Sahu,[22] S. Salur,[43] J. Sandweiss,[60] J. Schambach,[52] A. M. Schmah,[27] W. B. Schmidke,[5] N. Schmitz,[29]
B. R. Schweid,[49] F. Seck,[14] J. Seger,[12] M. Sergeeva,[8] R. Seto,[9] P. Seyboth,[29] N. Shah,[47] E. Shahaliev,[24]
P. V. Shanmuganathan,[28] M. Shao,[45] F. Shen,[46] W. Q. Shen,[47] S. S. Shi,[10] Q. Y. Shou,[47] E. P. Sichtermann,[27]
S. Siejka,[58] R. Sikora,[2] M. Simko,[34] JSingh,[37] S. Singha,[25] D. Smirnov,[5] N. Smirnov,[60] W. Solyst,[20] P. Sorensen,[5]
H. M. Spinka,[4] B. Srivastava,[40] T. D. S. Stanislaus,[56] D. J. Stewart,[60] M. Strikhanov,[31] B. Stringfellow,[40]
A. A. P. Suaide,[44] T. Sugiura,[54] M. Sumbera,[34] B. Summa,[38] X. M. Sun,[10] X. Sun,[10] Y. Sun,[45] B. Surrow,[50]
D. N. Svirida,[3] P. Szymanski,[58] A. H. Tang,[5] Z. Tang,[45] A. Taranenko,[31] T. Tarnowsky,[30] J. H. Thomas,[27]
A. R. Timmins,[19] D. Tlusty,[42] T. Todoroki,[5] M. Tokarev,[24] C. A. Tomkiel,[28] S. Trentalange,[8] R. E. Tribble,[51]
P. Tribedy,[5] S. K. Tripathy,[22] O. D. Tsai,[8] B. Tu,[10] T. Ullrich,[5] D. G. Underwood,[4] I. Upsal,[5, 46] G. Van Buren,[5]
J. Vanek,[34] A. N. Vasiliev,[39] I. Vassiliev,[16] F. Videbæk,[5] S. Vokal,[24] S. A. Voloshin,[59] A. Vossen,[20]
F. Wang,[40] G. Wang,[8] P. Wang,[45] Y. Wang,[10] Y. Wang,[53] J. C. Webb,[5] L. Wen,[8] G. D. Westfall,[30]
H. Wieman,[27] S. W. Wissink,[20] R. Witt,[55] Y. Wu,[25] Z. G. Xiao,[53] G. Xie,[11] W. Xie,[40] J. Xu,[10] N. Xu,[27]
Q. H. Xu,[46] Y. F. Xu,[47] Z. Xu,[5] C. Yang,[46] Q. Yang,[46] S. Yang,[5] Y. Yang,[33] Z. Ye,[11] Z. Ye,[11] L. Yi,[46] K. Yip,[5]
I. -K. Yoo,[41] N. Yu,[10] H. Zbroszczyk,[58] W. Zha,[45] J. Zhang,[27] J. Zhang,[21] L. Zhang,[10] S. Zhang,[45] S. Zhang,[47]
X. P. Zhang,[53] Y. Zhang,[45] Z. Zhang,[47] J. Zhao,[40] C. Zhong,[47] C. Zhou,[47] X. Zhu,[53] Z. Zhu,[46] and M. Zyzak[16]

(STAR Collaboration)

[1] *Abilene Christian University, Abilene, Texas 79699*
[2] *AGH University of Science and Technology, FPACS, Cracow 30-059, Poland*
[3] *Alikhanov Institute for Theoretical and Experimental Physics, Moscow 117218, Russia*

[4] *Argonne National Laboratory, Argonne, Illinois 60439*
[5] *Brookhaven National Laboratory, Upton, New York 11973*
[6] *University of California, Berkeley, California 94720*
[7] *University of California, Davis, California 95616*
[8] *University of California, Los Angeles, California 90095*
[9] *University of California, Riverside, California 92521*
[10] *Central China Normal University, Wuhan, Hubei 430079*
[11] *University of Illinois at Chicago, Chicago, Illinois 60607*
[12] *Creighton University, Omaha, Nebraska 68178*
[13] *Czech Technical University in Prague, FNSPE, Prague 115 19, Czech Republic*
[14] *Technische Universität Darmstadt, Darmstadt 64289, Germany*
[15] *Eötvös Loránd University, Budapest, Hungary H-1117*
[16] *Frankfurt Institute for Advanced Studies FIAS, Frankfurt 60438, Germany*
[17] *Fudan University, Shanghai, 200433*
[18] *University of Heidelberg, Heidelberg 69120, Germany*
[19] *University of Houston, Houston, Texas 77204*
[20] *Indiana University, Bloomington, Indiana 47408*
[21] *Institute of Modern Physics, Chinese Academy of Sciences, Lanzhou, Gansu 730000*
[22] *Institute of Physics, Bhubaneswar 751005, India*
[23] *University of Jammu, Jammu 180001, India*
[24] *Joint Institute for Nuclear Research, Dubna 141 980, Russia*
[25] *Kent State University, Kent, Ohio 44242*
[26] *University of Kentucky, Lexington, Kentucky 40506-0055*
[27] *Lawrence Berkeley National Laboratory, Berkeley, California 94720*
[28] *Lehigh University, Bethlehem, Pennsylvania 18015*
[29] *Max-Planck-Institut für Physik, Munich 80805, Germany*
[30] *Michigan State University, East Lansing, Michigan 48824*
[31] *National Research Nuclear University MEPhI, Moscow 115409, Russia*
[32] *National Institute of Science Education and Research, HBNI, Jatni 752050, India*
[33] *National Cheng Kung University, Tainan 70101*
[34] *Nuclear Physics Institute AS CR, Prague 250 68, Czech Republic*
[35] *Ohio State University, Columbus, Ohio 43210*
[36] *Institute of Nuclear Physics PAN, Cracow 31-342, Poland*
[37] *Panjab University, Chandigarh 160014, India*
[38] *Pennsylvania State University, University Park, Pennsylvania 16802*
[39] *Institute of High Energy Physics, Protvino 142281, Russia*
[40] *Purdue University, West Lafayette, Indiana 47907*
[41] *Pusan National University, Pusan 46241, Korea*
[42] *Rice University, Houston, Texas 77251*
[43] *Rutgers University, Piscataway, New Jersey 08854*
[44] *Universidade de São Paulo, São Paulo, Brazil 05314-970*
[45] *University of Science and Technology of China, Hefei, Anhui 230026*
[46] *Shandong University, Qingdao, Shandong 266237*
[47] *Shanghai Institute of Applied Physics, Chinese Academy of Sciences, Shanghai 201800*
[48] *Southern Connecticut State University, New Haven, Connecticut 06515*
[49] *State University of New York, Stony Brook, New York 11794*
[50] *Temple University, Philadelphia, Pennsylvania 19122*
[51] *Texas A&M University, College Station, Texas 77843*
[52] *University of Texas, Austin, Texas 78712*
[53] *Tsinghua University, Beijing 100084*
[54] *University of Tsukuba, Tsukuba, Ibaraki 305-8571, Japan*
[55] *United States Naval Academy, Annapolis, Maryland 21402*
[56] *Valparaiso University, Valparaiso, Indiana 46383*
[57] *Variable Energy Cyclotron Centre, Kolkata 700064, India*
[58] *Warsaw University of Technology, Warsaw 00-661, Poland*
[59] *Wayne State University, Detroit, Michigan 48201*
[60] *Yale University, New Haven, Connecticut 06520*
(Dated: March 26, 2019)

The first (v_1^{fluc}), second (v_2) and third (v_3) harmonic coefficients of the azimuthal particle distribution at mid-rapidity, are extracted for charged hadrons and studied as a function of transverse momentum (p_T) and mean charged particle multiplicity density $\langle N_{ch} \rangle$ in U+U ($\sqrt{s_{NN}} = 193$ GeV), Au+Au, Cu+Au, Cu+Cu, d+Au and p+Au collisions at $\sqrt{s_{NN}} = 200$ GeV with the STAR Detector. For the same $\langle N_{ch} \rangle$, the v_1^{fluc} and v_3 coefficients are observed to be independent of collision system,

while v_2 exhibits such a scaling only when normalized by the initial-state eccentricity (ε_2). The data also show that $\ln(v_2/\varepsilon_2)$ scales linearly with $\langle N_{ch}\rangle^{-1/3}$. These measurements provide insight into initial-geometry fluctuations and the role of viscous hydrodynamic attenuation on v_n from small to large collision systems.

PACS numbers: 25.75.-q, 25.75.Gz, 25.75.Ld

An important goal of the experimental program at the Relativistic Heavy Ion Collider (RHIC) at Brookhaven National Laboratory (BNL), is to provide quantitative experimental data which can (i) give insight on the dynamical evolution of the quark-gluon plasma (QGP) created in heavy ion collisions, and (ii) serve as important constraints for the extraction of the associated transport coefficients. The azimuthal anisotropy of particle emission in the transverse plane, known as anisotropic flow, is a key observable because it reflects the viscous hydrodynamic response to the initial spatial distribution in energy density (both from intrinsic geometry and fluctuations), produced in the early stages of the collision [1–15].

Experimentally, anisotropic flow manifests as an azimuthal asymmetry of the measured single-particle distribution, quantified by the complex flow coefficients [9, 13, 16]:

$$V_n \equiv v_n e^{in\Psi_n} = \left\langle e^{in\phi} \right\rangle, \qquad (1)$$

where v_n characterizes the magnitude of the azimuthal anisotropy of the particle spectrum in the transverse direction, Ψ_n is the event-plane and the single brackets denote an average with respect to the single-particle spectrum in a collision event. The event-by-event fluctuations in the initial state density profile result in fluctuations of both the generated paricle spectrum and V_n. The first three coefficients, v_1, v_2, and v_3, are termed directed, elliptic, and triangular flow, respectively. The fluctuations-driven component of v_1, termed $v_1^{\rm fluc}$, is proportional to the dipole asymmetry of the collision system [17, 18].

The v_n coefficients are also related to the Fourier coefficients v_{nn} which characterize the amplitude of the two-particle correlations in relative azimuthal angle $\Delta\phi = \phi_a - \phi_b$ [19, 20] for the particles a and b, which comprise the pairs:

$$\frac{dN^{pairs}}{d\Delta\phi} \propto 1 + 2\sum_{n=1}^{\infty} v_{nn}\cos(n\Delta\phi),$$
$$v_{nn}(p_T^a, p_T^b) = v_n(p_T^a)v_n(p_T^b) + \delta_{NF}, \qquad (2)$$

where $\delta_{\rm NF}$ signify the contributions of short-range non-flow correlations due to resonance decays, Bose-Einstein correlations and jet-like decays, as well as long-range contributions which result from momentum conservation [18, 20–22].

The initial anisotropic density profile $\rho_e(r,\varphi)$ in the transverse ($\perp$) plane, which drives anisotropic flow, can

be similarly characterized by complex eccentricity coefficients [17, 23–26]:

$$\mathcal{E}_n \equiv \varepsilon_n e^{in\Phi_n} = -\frac{\int d^2 r_\perp \, r^m \, e^{in\varphi} \, \rho_e(r,\varphi)}{\int d^2 r_\perp \, r^m \, \rho_e(r,\varphi)}, \qquad (3)$$

where Φ_n is the angle of the so-called n^{th}-order participant plane; $m = n$ for $n \geq 2$ and $m = 3$ for $n = 1$ [17]. Theoretical investigations show that $v_n \propto \varepsilon_n$ for elliptic and triangular flow ($n = 2,3$) [26–29], and the temperature (T) dependent specific shear viscosity $\frac{\eta}{s}(T)$, of the created medium, reduces the ratio v_n/ε_n. Thus, the comparison of viscous hydrodynamical model calculations to this ratio is commonly employed to estimate $\frac{\eta}{s}(T)$ and its average $\left\langle \frac{\eta}{s}(T) \right\rangle$, over the system's evolution [5, 8, 10, 12, 14, 26, 30–34]. The viscous attenuation of v_n/ε_n can also be understood within an acoustic model framework, akin to that for viscous relativistic hydrodynamics [35–41]:

$$\ln(v_n/\varepsilon_n) \propto -n^2 \left\langle \frac{\eta}{s}(T) \right\rangle \langle N_{ch}\rangle^{-1/3}, \qquad (4)$$

where $\langle N_{ch}\rangle$ is the charged particle multiplicity density and $\langle N_{ch}\rangle^{-1/3}$ is a proxy for the dimensionless size of the system [35, 36, 42].

Measurements at both RHIC and the Large Hadron Collider (LHC), have indicated sizable v_2 and v_3 values in high multiplicity $p + p$ [43, 44], d+Au [45–49] and p+Pb collisions [50–52], reminiscent of those observed in medium and large A+A collisions [53]. These measurements have generated considerable debate on whether the final-state collective effects, which dominate the mechanism for anisotropic flow in A+A collisions, also drive the anisotropy measured in high-multiplicity $p + p$ and p+A (d+A) collisions [35, 36, 54–57]. The related question of whether the properties of the medium produced in the small $p + p$, p+A and d+A [36, 45] systems are similar to those produced in the larger A+A systems is also not fully settled.

In this letter we present and compare a comprehensive set of $v_1^{\rm fluc}$, v_2 and v_3 measurements for U+U ($\sqrt{s_{NN}} = 193$ GeV), Au+Au, Cu+Cu, Cu+Au, d+Au, and p+Au collisions at $\sqrt{s_{NN}} = 200$ GeV, that should prove invaluable for the interpretation of collectivity in small systems, and in ongoing efforts to constrain theoretical models and obtain a robust extraction of $\frac{\eta}{s}(T)$.

The data for the six colliding systems presented in this work, were collected with the STAR detector at RHIC using a minimum-bias trigger [58]. Charged-particle tracks, measured in the full azimuth and pseudorapidity range
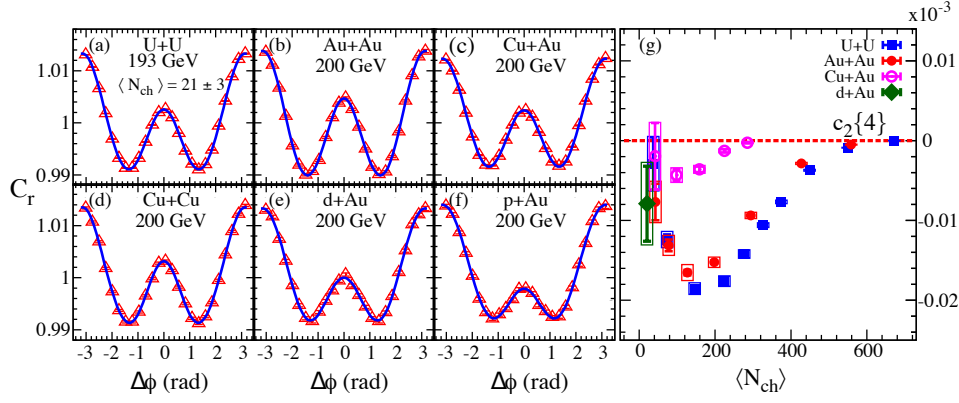
Fig. 1. Two-particle azimuthal correlation functions (a-f) and four-particle cumulants (g) for p_T-integrated track pairs $(-1 \lesssim \eta \lesssim 1)$. Results are shown for U+U (a) collisions ($\sqrt{s_{NN}} = 193$ GeV) and Au+Au (b), Cu+Au (c), Cu+Cu (d), d+Au (e) and p+Au (f) collisions ($\sqrt{s_{NN}} = 200$ GeV) for $\langle N_{ch} \rangle = 21 \pm 3$. The solid curves show the result of a Fourier fit to the data. Panel (g) shows the second-order cumulant $c_2\{4\}$ vs. $\langle N_{ch} \rangle$, obtained with the three sub-events method for the same data sets.

($|\eta| < 1.0$) of the Time Projection Chamber (TPC) [59], were used to reconstruct the collision vertices. Events were selected with vertex positions ± 30 cm from the nominal center of the TPC (in the beam direction).

Collision centrality and the associated $\langle N_{ch} \rangle$ were determined from the measured event-by-event multiplicity with the aid of a tuned Monte Carlo Glauber calculation [60]. Analyzed tracks were required to have a distance of closest approach to the primary vertex of less than 3 cm, and have at least 15 TPC space points used in their reconstruction. To remove split tracks, the ratio of the number of fit points to a maximum possible number of TPC space points was required to be larger than 0.52. Analyzed tracks were restricted to $0.2 < p_T < 4$ GeV/c.

Two-particle $\Delta\phi$ correlation functions (C_r) were generated to extract the flow coefficients:

$$C_r(\Delta\phi, \Delta\eta) = \frac{(dN/d\Delta\phi)_{\text{same}}}{(dN/d\Delta\phi)_{\text{mixed}}}, \qquad (5)$$

where $(dN/d\Delta\phi)_{\text{same}}$ represents the distribution of track pairs, in relative azimuthal angle $\Delta\phi$, taken from the same event. $(dN/d\Delta\phi)_{\text{mixed}}$ represents the $\Delta\phi$ distribution for track pairs in which each member is selected from different events in the same $\langle N_{ch} \rangle$ and 5 cm vertex position classes. Following detailed studies of the influence of possible non-flow contributions, the pseudorapidity requirement $|\Delta\eta| > 0.7$ was imposed for all track pairs to suppress such contributions [61]. A further check for the dominance of flow correlations was obtained by measuring the second-order four-particle cumulant $c_2\{4\}$:

$$c_2\{4\} = \langle\langle 4 \rangle\rangle - 2\langle\langle 2 \rangle\rangle^2, \qquad (6)$$

where $\langle\langle \rangle\rangle$ represents the averaging first over particles in an event and then over all events within a given event class. The three sub-events method [62] was used for these evaluations with sub-events for $\eta_1 < -0.35$, $|\eta_2| < 0.35$ and $\eta_3 > 0.35$.

Figures 1(a-f) show the correlation functions obtained for U+U, Au+Au, Cu+Au, Cu+Cu, d+Au and p+Au collisions for $\langle N_{ch} \rangle = 21 \pm 3$. They indicate patently similar correlation patterns with a visible enhancement of near-side ($\Delta\phi \sim 0$) pairs, reminiscent of the so-called "ridge" observed in high multiplicity $p+p$ [43, 44], d+Au [47, 48] and p+Pb collisions [50, 52]. The corresponding values for $c_2\{4\}$ vs. $\langle N_{ch} \rangle$, shown in Fig. 1 (g), indicate negative values which suggests the absence of significant short-range non-flow contributions, and the dominance of flow correlations to C_r [63, 64]. Note that the paucity of central p+Au events precluded the extraction of $c_2\{4\}$ from these events.

Similar sets of correlation functions were generated as a function of p_T and $\langle N_{ch} \rangle$ to allow a study of v_1^{fluc}, v_2 and v_3 (for each collision system) for different dimensionless sizes and eccentricities. Monte Carlo quark Glauber (MC-qGlauber) calculations [35] were used to compute ε_n as a function of collision centrality or $\langle N_{ch} \rangle$ for all collision systems, from the two-dimensional profile of the density of quark participants in the transverse plane (c.f Eq. 3). The model takes account of the finite size of the nucleon, the wounding profile of the nucleon, the distribution of quarks inside the nucleon, and quark cross sections which reproduce the NN inelastic cross section at $\sqrt{s_{NN}} = 200$ GeV; all are constrained by experimental measurements. A systematic uncertainty of 2-5% was estimated for the eccentricities from variations of the model parameters.

The v_{nn} coefficients were obtained from the correlation function as:

$$v_{nn} = \frac{\sum_{\Delta\phi} C_r(\Delta\phi, \Delta\eta)\cos(n\Delta\phi)}{\sum_{\Delta\phi} C_r(\Delta\phi, \Delta\eta)}, \qquad (7)$$

and then used to extract v_n for $n > 1$,

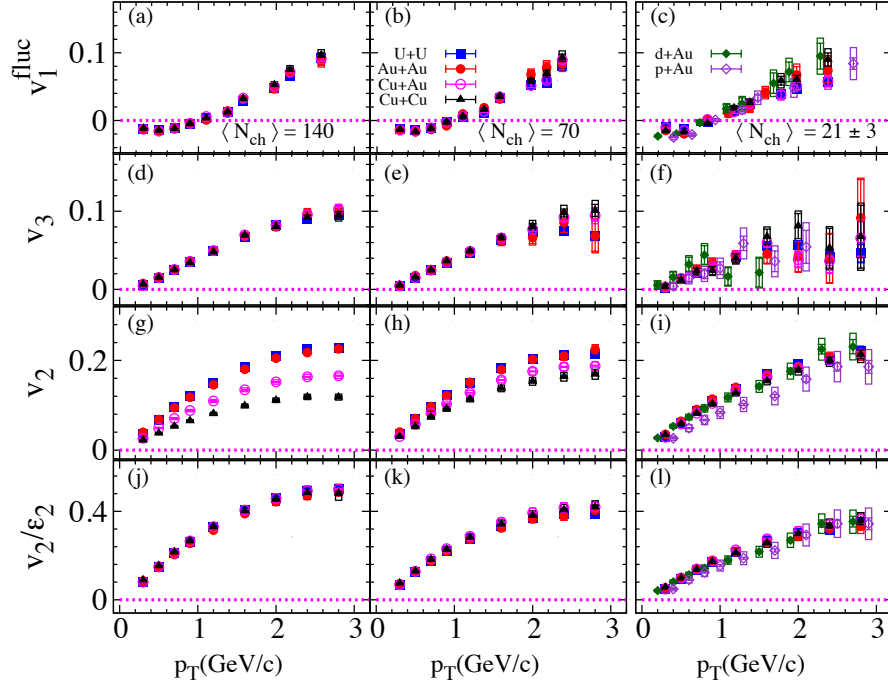$$v_{nn}(p_T^a, p_T^b) = v_n(p_T^a)v_n(p_T^b), \qquad (8)$$

Fig. 2. v_1^{fluc}, v_2, v_3 and v_2/ε_2 vs. p_T for several $\langle N_{ch} \rangle$ selections. Results are compared for U+U, Au+Au, Cu+Au and Cu+Cu for $\langle N_{ch} \rangle = 140$, and $\langle N_{ch} \rangle = 70$ and for U+U, Au+Au, Cu+Au, Cu+Cu, d+Au and p+Au for $\langle N_{ch} \rangle = 21 \pm 3$. For the latter, the p+Au and d+Au data points are shifted by 0.1 GeV/c and -0.1 GeV/c (respectively) to aid clarity.

and the v_1^{fluc} component of v_1,

$$v_{11}(p_T^a, p_T^b) = v_1^{\text{fluc}}(p_T^a)v_1^{\text{fluc}}(p_T^b) - Kp_T^a p_T^b, \quad (9)$$

where $K \propto 1/(\langle N_{ch} \rangle \langle p_T^2 \rangle)$ takes account of the long-range non-flow correlations induced by global momentum conservation [21, 22, 61]. A simultaneous fit of $v_{11}(p_T^b)$ for several selections of p_T^a (c.f. Eq. 9) was used to facilitate the extraction of v_1^{fluc} [61].

The systematic uncertainties associated with the v_n extractions were estimated through studies of the influence of the choice of the cuts for z-vertex position, track selection, efficiency correction, $\Delta\eta$ and the fitting procedure. The uncertainty associated with $\Delta\eta$ dominate for the d+Au and p+Au systems. The respective uncertainties, ranging from 2% to 10%, were added in quadrature to obtain an overall systematic uncertainty for the respective measurements.

The extracted values of $v_1^{\text{fluc}}(p_T)$, $v_2(p_T)$ and $v_3(p_T)$ for the collision systems are compared in Fig. 2 for different values of $\langle N_{ch} \rangle$. Figures 2(a) - 2(c) indicate similar $v_1^{\text{fluc}}(p_T)$ magnitudes for the systems specified at each $\langle N_{ch} \rangle$, as well as the characteristic pattern of a change from negative $v_1^{\text{fluc}}(p_T)$ at low-p_T to positive $v_1^{\text{fluc}}(p_T)$ for $p_T \gtrsim 1$ GeV/c. This pattern confirms the predicted trends for dipolar flow [17, 18, 21, 61] and further indicates that for the selected values of $\langle N_{ch} \rangle$, $v_1^{\text{fluc}}(p_T)$ is essentially independent of collision system. Figures 2(d) - 2(f), show similar system-independent patterns for $v_3(p_T)$, but with magnitudes and trends that differ from those for $v_1^{\text{fluc}}(p_T)$. The system independence of $v_1^{\text{fluc}}(p_T)$

and $v_3(p_T)$ for the indicated $\langle N_{ch} \rangle$ values suggests that the fluctuations-driven initial-state eccentricities ε_1 and ε_3, and the subsequent final-state interactions are similar for the indicated collision systems.

The $v_2(p_T)$ values shown in Figs. 2(g) - 2(i) contrasts with those for $v_1^{\text{fluc}}(p_T)$ and $v_3(p_T)$. That is, the trends for a given $\langle N_{ch} \rangle$ are independent of the collision system, but the magnitudes are not system-independent, albeit with differences that grow with $\langle N_{ch} \rangle$. The system dependent differences, apparent for $\langle N_{ch} \rangle = 140$ and 70 (Figs. 2(g) and 2(h)), can be attributed to the system-dependent ε_2 values for each $\langle N_{ch} \rangle$. For $\langle N_{ch} \rangle \sim 21$ (Fig. 2(i)), the MC-qGlauber eccentricities for the different systems, do not vary strongly.

Figures 2(j) and 2(k) confirm the influence of the system-dependent ε_2 values for $\langle N_{ch} \rangle = 140$ and 70 . That is, they show data collapse onto a single curve for v_2/ε_2 vs. p_T for U+U, Au+Au, Cu+Au and Cu+Cu systems. Fig. 2(l) also indicates an approximate collapse of the scaled results for p+Au and d+Au onto the curve for the eccentricity-scaled A+A data. This pattern is suggestive of a dominant collective flow contribution to the measured anisotropy in high multiplicity p+A(d+A) collisions [36]. However, a quantitative estimate of a possible long-range non-flow contribution is required to fully establish the degree of this apparent scaling.

The $\langle N_{ch} \rangle$ dependence of v_1^{fluc}, v_2, and v_3 are compared for all six collision systems in Figs. 3(a) - 3(c); they are in good agreement with the v_2 data reported for U+U and Au+Au collisions in Ref. [66]. The inset in Fig. 3(a) compares the associated values of K vs. $\langle N_{ch} \rangle^{-1}$ (c.f.
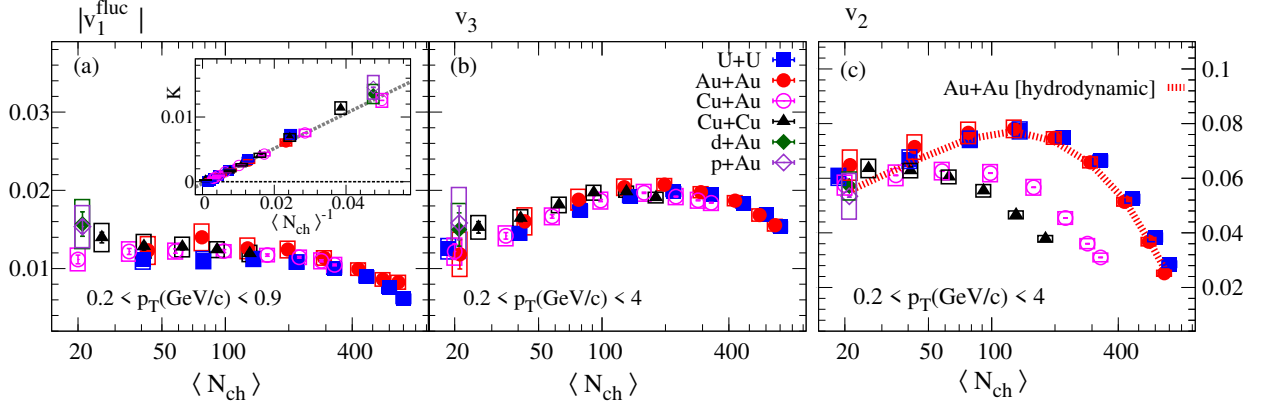
Fig. 3. Comparison of the $\langle N_{ch} \rangle$ dependence of v_1^{fluc} (a), v_3 (b) and v_2 (c) for all collision systems for the p_T selections indicated. The dashed curve in (c) represent a hydrodynamic model calculation [65] for Au+Au collisions. The $\langle N_{ch} \rangle$ values for p+Au and d+Au correspond to $\sim$ 0-20% central collisions. The inset in (a) compares the extracted values of K vs. $\langle N_{ch} \rangle^{-1}$ for each system; the dashed line is drawn to guide the eye.

Eq. 9) for each system.

For $\langle N_{ch} \rangle \gtrsim 170$, the v_n values all show a decrease with increasing values of $\langle N_{ch} \rangle$, consistent with the expected decrease of ε_n as collisions become more central. The apparent decrease in the values of v_2 for $\langle N_{ch} \rangle \lesssim 170$ corroborate the dominant role of size-driven viscous attenuation of the flow harmonics for these multiplicities. Note that ε_2 increases for $\langle N_{ch} \rangle < 170$. Figures 3(a) and 3(b) indicate system-independent magnitudes and trends for v_1^{fluc} and v_3 analogous to the p_T-dependent results shown in Fig. 2.

The v_2 comparisons shown in Fig. 3(c), accentuate the system-dependent patterns observed in Figs. 2(g), 2(h) and 2(i). Here, the uncertainties for the p+Au and d+Au data points for $\langle N_{ch} \rangle \sim 21$, reflect the systematic uncertainty estimates for residual non-flow contributions which are smaller for these p_T-integrated measurements. The dashed curve indicates good agreement between the data and a hydrodynamic calculation for Au+Au collisions [65].

The striking system-dependent patterns shown in Fig. 3(c) can be attributed to the strong dependence of ε_2 on system size for a fixed value of $\langle N_{ch} \rangle$. This shape dependence, which weakens for low $\langle N_{ch} \rangle$, is confirmed via the plot of v_2/ε_2 vs. $\langle N_{ch} \rangle^{-1/3}$ shown in Fig. 4. A similar plot, reflecting the n^2 dependence of viscous attenuation [35, 36], was obtained for v_3/ε_3 vs. $\langle N_{ch} \rangle^{-1/3}$. The inset in Fig. 4 indicates a marked similarity between the slopes of the eccentricity-scaled v_2 for U+U, Au+Au, Cu+Au and Cu+Cu collisions over the indicated multiplicity range. The eccentricity-scaled results for d+Au and p+Au also follow the data trend for these heavier collision species [46, 67] with larger systematic uncertainty. Hydrodynamic simulations for Au+Au collisions [65] exhibit similar scaling trends within the same range of $\langle N_{ch} \rangle$.
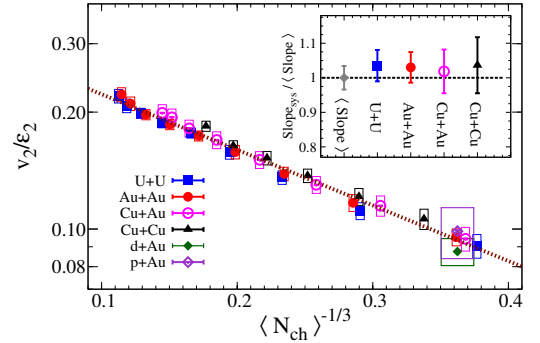
In summary, we have used the two-particle correlation

Fig. 4. v_2/ε_2 vs. $\langle N_{ch} \rangle^{-1/3}$ for U+U, Au+Au, Cu+Au, Cu+Cu, d+Au and p+Au collisions as indicated. The open boxes indicate systematic uncertainties. The v_2 data is the same as in Fig. 3(c). The dotted line represents an exponential fit to the data with Eq. 4. The inset shows the respective ratios of the slopes extracted for each system relative to the slope extracted from a fit to the combined data sets ($\langle Slope \rangle$ = $8.2 \times 10^{-1} \pm 0.02$).

method to carry out a comprehensive set of measurements of v_1^{fluc}, v_2, and v_3 as a function of p_T and $\langle N_{ch} \rangle$ in U+U ($\sqrt{s_{NN}}$ = 193 GeV) and Au+Au, Cu+Au, Cu+Cu, d+Au, and p+Au collisions at $\sqrt{s_{NN}}$ = 200 GeV. The detailed comparisons of the measurements highlight the sensitivity of v_n to the magnitude of the initial-state eccentricity, system size and the final-state interactions in the expanding matter. The wealth of the A+A measurements lead to data collapse of $\ln(v_n/\varepsilon_n)$ vs. $\langle N_{ch} \rangle^{-1/3}$ onto a single curve. Similarly scaled results for d+Au and p+Au (for $\langle N_{ch} \rangle \sim 21$) are also observed with larger uncertainty. The combined measurements and their scaling properties provide a new set of constraints which could prove invaluable for the interpretation of collectivity in small systems and for detailed theoretical extraction of the temperature-dependent $\frac{\eta}{s}$.

———————

[1] P. Danielewicz *et al.*, Phys. Rev. Lett. **81**, 2438 (1998), arXiv:nucl-th/9803047 [nucl-th].

[2] K. H. Ackermann *et al.* (STAR), Phys. Rev. Lett. **86**, 402 (2001), arXiv:nucl-ex/0009011 [nucl-ex].

[3] K. Adcox *et al.* (PHENIX), Phys. Rev. Lett. **89**, 212301 (2002), arXiv:nucl-ex/0204005 [nucl-ex].

[4] U. Heinz and P. Kolb, Nucl. Phys. **A702**, 269 (2002).

[5] T. Hirano, U. W. Heinz, D. Kharzeev, R. Lacey, and Y. Nara, Phys.Lett. **B636**, 299 (2006), arXiv:nucl-th/0511046 [nucl-th].

[6] P. Huovinen, P. F. Kolb, U. W. Heinz, P. V. Ruuskanen, and S. A. Voloshin, Phys. Lett. **B503**, 58 (2001).

[7] T. Hirano and K. Tsuda, Phys. Rev. **C66**, 054905 (2002), arXiv:nucl-th/0205043.

[8] P. Romatschke and U. Romatschke, Phys.Rev.Lett. **99**, 172301 (2007), arXiv:0706.1522 [nucl-th].

[9] M. Luzum, J. Phys. **G38**, 124026 (2011), arXiv:1107.0592 [nucl-th].

[10] H. Song, S. A. Bass, U. Heinz, T. Hirano, and C. Shen, Phys. Rev. Lett. **106**, 192301 (2011), [Erratum: Phys. Rev. Lett.109,139904(2012)], arXiv:1011.2783 [nucl-th].

[11] J. Qian, U. W. Heinz, and J. Liu, Phys. Rev. **C93**, 064901 (2016), arXiv:1602.02813 [nucl-th].

[12] B. Schenke, S. Jeon, and C. Gale, Phys.Lett. **B702**, 59 (2011), arXiv:1102.0575 [hep-ph].

[13] D. Teaney and L. Yan, Phys. Rev. **C86**, 044908 (2012), arXiv:1206.1905 [nucl-th].

[14] F. G. Gardim, F. Grassi, M. Luzum, and J.-Y. Ollitrault, Phys.Rev.Lett. **109**, 202302 (2012), arXiv:1203.2882 [nucl-th].

[15] R. A. Lacey *et al.*, J. Phys. **G43**, 10LT01 (2016), arXiv:1311.1728 [nucl-ex].

[16] A. Bilandzic, R. Snellings, and S. Voloshin, Phys. Rev. **C83**, 044913 (2011), arXiv:1010.0233 [nucl-ex].

[17] D. Teaney and L. Yan, Phys. Rev. **C83**, 064904 (2011), arXiv:1010.1876 [nucl-th].

[18] M. Luzum and J.-Y. Ollitrault, Phys. Rev. Lett. **106**, 102301 (2011), arXiv:1011.6361 [nucl-ex].

[19] A. M. Poskanzer and S. A. Voloshin, Phys. Rev. **C58**, 1671 (1998), arXiv:nucl-ex/9805001 [nucl-ex].

[20] R. A. Lacey, Nucl. Phys. **A774**, 199 (2006), arXiv:nucl-ex/0510029 [nucl-ex].

[21] E. Retinskaya, M. Luzum, and J.-Y. Ollitrault, Phys. Rev. Lett. **108**, 252302 (2012), arXiv:1203.0931 [nucl-th].

[22] G. Aad *et al.* (ATLAS), Phys. Rev. **C86**, 014907 (2012), arXiv:1203.3087 [hep-ex].

[23] B. H. Alver, C. Gombeaud, M. Luzum, and J.-Y. Ollitrault, Phys. Rev. **C82**, 034913 (2010), arXiv:1007.5469 [nucl-th].

[24] H. Petersen, G.-Y. Qin, S. A. Bass, and B. Muller, Phys. Rev. **C82**, 041901 (2010), arXiv:1008.0625 [nucl-th].

[25] R. A. Lacey, R. Wei, N. N. Ajitanand, and A. Taranenko, Phys. Rev. **C83**, 044902 (2011), arXiv:1009.5230 [nucl-ex].

[26] Z. Qiu and U. W. Heinz, Phys. Rev. **C84**, 024911 (2011), arXiv:1104.0650 [nucl-th].

[27] J. Fu, Phys. Rev. **C92**, 024904 (2015).

[28] H. Niemi, K. J. Eskola, and R. Paatelainen, Phys. Rev. **C93**, 024907 (2016), arXiv:1505.02677 [hep-ph].

[29] J. Noronha-Hostler, L. Yan, F. G. Gardim, and J.-Y. Ollitrault, Phys. Rev. **C93**, 014909 (2016), arXiv:1511.03896 [nucl-th].

[30] B. Schenke, S. Jeon, and C. Gale, Phys.Rev.Lett. **106**, 042301 (2011), arXiv:1009.3244 [hep-ph].

[31] P. Bozek, M. Chojnacki, W. Florkowski, and B. Tomasik, Phys.Lett. **B694**, 238 (2010), arXiv:1007.2294 [nucl-th].

[32] H. Niemi, G. Denicol, P. Huovinen, E. Molnar, and D. Rischke, Phys. Rev. **C86**, 014909 (2012), arXiv:1203.2452 [nucl-th].

[33] S. McDonald, C. Shen, F. Fillion-Gourdeau, S. Jeon, and C. Gale, Phys. Rev. **C95**, 064913 (2017), arXiv:1609.02958 [hep-ph].

[34] J. E. Bernhard, J. S. Moreland, S. A. Bass, J. Liu, and U. Heinz, Phys. Rev. **C94**, 024907 (2016), arXiv:1605.03954 [nucl-th].

[35] P. Liu and R. A. Lacey, Phys. Rev. **C98**, 021902 (2018), arXiv:1802.06595 [nucl-ex].

[36] P. Liu and R. A. Lacey, Phys. Rev. **C98**, 031901 (2018), arXiv:1804.04618 [nucl-ex].

[37] R. A. Lacey *et al.*, (2013), arXiv:1301.0165 [nucl-ex].

[38] N. Magdy (STAR), PoS **CPOD2017**, 005 (2018), arXiv:1801.07872 [nucl-ex].

[39] N. Magdy (STAR), J. Phys. Conf. Ser. **779**, 012060 (2017).

[40] E. Shuryak and I. Zahed, Phys. Rev. **C88**, 044915 (2013), arXiv:1301.4470 [hep-ph].

[41] R. A. Lacey, A. Taranenko, N. N. Ajitanand, and J. M. Alexander, (2011), arXiv:1105.3782 [nucl-ex].

[42] R. A. Lacey *et al.*, (2016), arXiv:1601.06001 [nucl-ex].

[43] V. Khachatryan *et al.* (CMS), Phys. Rev. Lett. **116**, 172302 (2016), arXiv:1510.03068 [nucl-ex].

[44] G. Aad *et al.* (ATLAS), Phys. Rev. Lett. **116**, 172301 (2016), arXiv:1509.04776 [hep-ex].

[45] J. Adams *et al.* (STAR), Phys. Rev. **C72**, 014904 (2005), arXiv:nucl-ex/0409033 [nucl-ex].

[46] A. Adare *et al.* (PHENIX), Phys. Rev. Lett. **111**, 212301 (2013), arXiv:1303.1794 [nucl-ex].

[47] A. Adare *et al.* (PHENIX), Phys. Rev. Lett. **114**, 192301 (2015), arXiv:1404.7461 [nucl-ex].

[48] L. Adamczyk *et al.* (STAR), Phys. Lett. **B743**, 333 (2015), arXiv:1412.8437 [nucl-ex].

[49] L. Adamczyk *et al.* (STAR), Phys. Lett. **B747**, 265 (2015), arXiv:1502.07652 [nucl-ex].

[50] S. Chatrchyan *et al.* (CMS), Phys. Lett. **B718**, 795 (2013), arXiv:1210.5482 [nucl-ex].

[51] B. Abelev *et al.* (ALICE), Phys. Lett. **B719**, 29 (2013), arXiv:1212.2001 [nucl-ex].

[52] G. Aad *et al.* (ATLAS), Phys. Rev. Lett. **110**, 182302 (2013), arXiv:1212.5198 [hep-ex].

[53] B. Alver *et al.* (PHOBOS), Phys. Rev. Lett. **98**, 242302 (2007), arXiv:nucl-ex/0610037 [nucl-ex].

[54] K. Dusling and R. Venugopalan, Phys. Rev. **D87**, 094034 (2013), arXiv:1302.7018 [hep-ph].

[55] P. Bozek and W. Broniowski, Phys. Rev. **C88**, 014903 (2013), arXiv:1304.3044 [nucl-th].

[56] K. Dusling, W. Li, and B. Schenke, Int. J. Mod. Phys. **E25**, 1630002 (2016), arXiv:1509.07939 [nucl-ex].

[57] C. Aidala *et al.* (PHENIX), Nature Phys. **15**, 214 (2019), arXiv:1805.02973 [nucl-ex].

[58] K. H. Ackermann *et al.* (STAR), Nucl. Instrum. Meth. **A499**, 624 (2003).

[59] M. Anderson *et al.*, Nucl. Instrum. Meth. **A499**, 659 (2003), arXiv:nucl-ex/0301015 [nucl-ex].

[60] L. Adamczyk *et al.* (STAR), Phys. Rev. **C86**, 054908 (2012), arXiv:1206.5528 [nucl-ex].

[61] J. Adam *et al.* (STAR), Phys. Lett. **B784**, 26 (2018), arXiv:1804.08647 [nucl-ex].

[62] J. Jia, M. Zhou, and A. Trzupek, Phys. Rev. **C96**, 034906 (2017), arXiv:1701.03830 [nucl-th].

[63] N. Borghini, P. M. Dinh, and J.-Y. Ollitrault, Phys. Rev. **C64**, 054901 (2001), arXiv:nucl-th/0105040 [nucl-th].

[64] W. Zhao, Y. Zhou, H. Xu, W. Deng, and H. Song, Phys. Lett. **B780**, 495 (2018), arXiv:1801.00271 [nucl-th].

[65] P. Alba *et al.*, Phys. Rev. **C98**, 034909 (2018), arXiv:1711.05207 [nucl-th].

[66] L. Adamczyk *et al.* (STAR), Phys. Rev. Lett. **115**, 222301 (2015), arXiv:1505.07812 [nucl-ex].

[67] C. Adler *et al.* (STAR), Phys. Rev. **C66**, 034904 (2002), arXiv:nucl-ex/0206001 [nucl-ex].